Interdiffusion and thermally induced strain relaxation in strained $Si_{1-x}Ge_x/Si$ superlattices

B. Holländer, R. Butz, and S. Mantl
Institut für Schicht- und Ionentechnik, Forschungszentrum Jülich, Postfach 1913, D-5170 Jülich, Germany
(Received 11 February 1992)

Thermal interdiffusion in five-period $Si/Si_{1-x}Ge_x$ superlattices with periods of 200 Å and Ge concentrations between $x=0.20$ and 0.70 was studied using Rutherford backscattering spectrometry in grazing-angle geometry. Both asymmetrically strained superlattices grown directly on Si, as well as symmetrically strained superlattices grown on relaxed $Si_{1-y}Ge_y$ buffer layers, were grown to compare the influence of the strain distribution on the interdiffusion. Rapid thermal annealing in the temperature range between 900 and 1125 °C leads to substantial interdiffusion indicated by a significant decrease of the amplitudes of the modulations of the backscattering yield. Interdiffusion coefficients were deduced using a Fourier algorithm. For a given Ge concentration x, the thermal dependence of the interdiffusion coefficients follows an Arrhenius law. The interdiffusivity increases with increasing Ge concentrations. An average activation energy for interdiffusion of ~4.0 eV was obtained. The elastic strain and the formation of crystal defects due to thermal treatment were investigated by He ion channeling.

INTRODUCTION

Epitaxial $Si/Si_{1-x}Ge_x$ heterostructures and superlattices gained widespread interest due to their promising applications in devices, e.g., Si/Ge heterobipolar transistors[1-3] and because of the indications for a quasidirect band gap in short-period superlattices.[4-6] Modulation-doped structures, e.g., the modulation-doped field-effect transistor attracted considerable attention because of the most recent progress in growing relaxed $Si_{1-y}Ge_y$ buffer layers with low dislocation densities. Using these fully relaxed buffer layers, record electron mobilities of more than 100 000 $cm^2/V\,s$ at 4.2 K were measured.[7,8] Regarding device applications, thermal stability of these lattice-mismatched heterostructures is a critical issue because high-temperature processing steps are often unavoidable during device fabrication. Thermal treatment can result in interdiffusion and strain relaxation, frequently by the formation of dislocations. As a consequence, the electronic properties, e.g., band alignment, may change.

The thermal stability of Si/SiGe superlattices and heterostructures has been investigated in several papers. However, most of these contributions concentrate on strain relaxation[1,9-14] and only few papers reported quantitative interdiffusion coefficients.[15-20] The effect of coherency strain on interdiffusion is still a controversial subject.[15,19-21] Also, the dependence on the Ge concentration has hardly been investigated.

In this paper we complete our previously published interdiffusion measurements on asymmetrically strained superlattices with various Ge concentrations.[22] Similar, nearly symmetrically strained superlattices with Ge concentrations between 20% and 70% were grown on $Si_{1-y}Ge_y$ buffer layers in order to investigate the influence of the elastic strain on the interdiffusion in the two types of superlattices. Elastic strain and dislocation densities were investigated by He ion channeling before and after annealing.

The epitaxial growth of $Si/Si_{1-x}Ge_x$ heterostructures is affected by the large lattice mismatch of 4.2% between Si and Ge. Depending on the Ge concentration, layer thickness, and growth temperature, the layered-structure growth is in either a pseudomorphic or a relaxed mode. Assuming Vegard's law, the lattice mismatch f between Si and $Si_{1-x}Ge_x$, with

$$f=(a_{\mathrm{SiGe}}-a_{\mathrm{Si}})/a_{\mathrm{Si}}\ ,$$

is given by $f=0.042x$. Due to the large lattice mismatch, the layer thickness, up to which pseudomorphic structures can be grown, is restricted to the so-called critical thickness.[23,24] At low growth temperatures, the layer structure is not in thermal equilibrium; therefore, pseudomorphic, metastable layers can be grown to thicknesses significantly larger than the thermal-equilibrium critical-layer thickness.[25] These metastable layers can relax by formation of dislocations during thermal treatment. Superlattices can relieve strain in two different ways: either each layer relaxes towards an unstrained state by the generation of misfit dislocations at each interface, or the complete structure shears as a unit with respect to the substrate by the formation of misfit dislocations only at the interface to the substrate.[26] In the case of asymmetrically strained, pseudomorphic superlattices grown on Si, only the $Si_{1-x}Ge_x$ layers are strained and, in addition, the total thickness of the superlattice is limited. The critical total-superlattice thickness is approximately given by the critical-layer thickness of a single alloy layer of the volume-averaged Ge concentration of the superlattice.[27] Symmetrically strained superlattices can be obtained using a relaxed $Si_{1-y}Ge_y$ buffer layer providing a virtual substrate with an intermediate lattice parameter. Following this idea, symmetrically strained superlattices can be grown in which the Si and $Si_{1-x}Ge_x$ layers are alternatingly under tensile and compressive strain.[28] For symmetrically strained superlattices, the total critical superlattice thick-

ness is, in principle, infinite.

The formation of crystal defects was investigated by He-ion channeling along the [100] sample normal. Tetragonal strain was measured by angular scanning along (100) planes through inclined [110] orientations.[29] In the case of pseudomorphic growth, the tetragonal strain is given by

$$\varepsilon_T \equiv \varepsilon_\perp - \varepsilon_\parallel = f\frac{(1+\nu)}{(1-\nu)} , \tag{1}$$

where $\varepsilon_\perp$ is the vertical strain, $\varepsilon_\parallel$ the in-plane strain, and ν Poisson's ratio. A pseudomorphic structure is characterized by a constant in-plane lattice parameter throughout the whole heterostructure, where the in-plane lattice parameter is determined by the substrate or by a relaxed buffer layer, which serves as a virtual substrate.

Interdiffusion coefficients were obtained by evaluating the decrease of the oscillation amplitudes of the measured Rutherford backscattering spectrometry (RBS) spectra after annealing using a Fourier algorithm.[30] In a periodic structure with period length H, the diffusion equation

$$\frac{\partial c}{\partial t} = D\nabla^2 c \tag{2}$$

is solved by a Fourier series

$$c = \frac{1}{2} + \sum_m \beta_m e^{-(2\pi m/H)^2 Dt} \sin\frac{2\pi m}{H} z , \tag{3}$$

with

$$\beta_m = \begin{cases} 2/(\pi m), & m = 1,3,5,\ldots \\ 0 \quad \text{otherwise.} \end{cases}$$

Except for the early stages of interdiffusion, the Fourier series can be approximated using only the sine term and neglecting all $m \geq 3$. The interdiffusion coefficients can be directly obtained from Eq. (3), since the annealing time is known and the period length and Ge concentrations before and after annealing are obtained from the amplitudes of the RBS spectra.

EXPERIMENT

The investigated samples consisted of five-period, nominally 100-Å Si/100-Å $Si_{1-x}Ge_x$ superlattices grown on Si(100) by molecular-beam epitaxy (MBE) at a substrate temperature of 550 °C in a Vacuum Generators VG90 MBE system. The asymmetrically strained superlattices were grown on a 1000-Å Si epilayer resulting in compressively strained $Si_{1-x}Ge_x$ layers and unstrained Si layers, as shown in Fig. 1. The symmetrically strained superlattices were grown on nearly relaxed $Si_{1-y}Ge_y$ buffer layers, which provide a virtual substrate with an in-plane lattice parameter between Si and $Si_{1-x}Ge_x$. The small amount of residual strain in the buffer layer is sketched in Fig. 1. In this case, the $Si_{1-x}Ge_x$ layers are compressively strained and the Si layers are under tensile strain. Asymmetrically strained superlattices with $x = 0.20$, 0.27, 0.45, 0.63, and 0.70 and symmetrically strained superlattices with $x = 0.20/y = 0.18$, $x = 0.28/y = 0.23$, $x = 0.46/y = 0.24$, and $x = 0.68/y = 0.37$ were used for

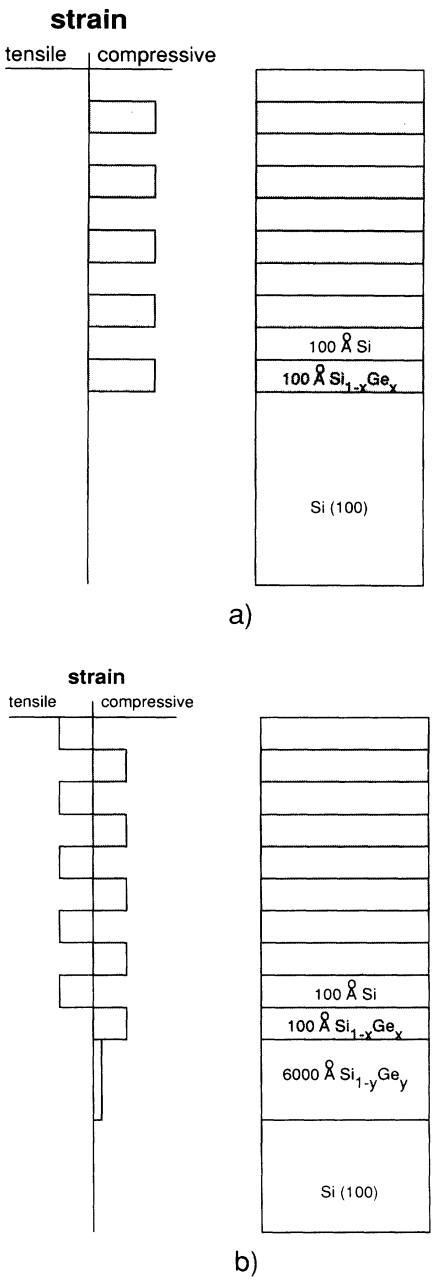

FIG. 1. Scheme of the structure and strain distribution of the investigated (a) asymmetrically and (b) symmetrically strained superlattices.

the interdiffusion measurements. For the investigated asymmetrically strained superlattices, the critical single-layer thickness is exceeded for Ge concentrations $x \geq 0.63$.[11] In the case of the asymmetrically strained superlattices, only the $Si_{1-x}Ge_x$ layers are strained; also, the total superlattice thickness has a limit, beyond which the superlattice will relax by dislocation formation. Also, the critical total superlattice thickness is expected to be exceeded for Ge concentrations larger than $x = 0.45$.[27]

Annealing was performed with a SITESA RMV4 rapid thermal processor, using 99.999% purity argon as process gas. Rutherford backscattering and channeling were

performed with 1.4-MeV He^+ ions and a scattering angle of 170°. In the case of grazing incidence, an angle of 81° and a diminutive beam divergence of less than ±0.015° were chosen. Tetragonal strain was obtained from the tilt angle between the [110] orientations of adjacent layers by angular scans along {100} planes through [110] orientations. The measurements were performed with a high-precision three-axis UHV goniometer.

RESULTS

Stoichiometry and layer thicknesses of the superlattices were determined from random RBS spectra. The angle of incidence of 81° was chosen to improve the depth resolution and the sample was continuously rotated around the sample normal during the measurement in order to avoid channeling effects. Figure 2 shows a spectrum of an asymmetrically strained superlattice with a Ge concentration of $x=0.27$ grown on Si(100), both before and after rapid thermal annealing at 1025 °C for 100 s. Surface backscattering energies of Si and Ge for 1.4-MeV He^+ ions are marked. The modulations of the backscattering yield from the five Si and $Si_{1-x}Ge_x$ layers are clearly visible. Dampening of the oscillation amplitudes with increasing depth can be ascribed to energy straggling of the ion beam. Layer thicknesses and stoichiometry were ascertained from the width and heights of the oscillation peaks by comparing the measured spectra with computer simulations using the RUMP code.[31]

Rapid thermal annealing leads to substantial interdiffusion between the individual layers of the superlattice indicated by a significant decrease of the amplitudes of the oscillations in the RBS spectrum in Fig. 2. Interdiffusion coefficients were obtained using the Fourier algorithm according to Eq. (3). The atomic concentrations and thus the elastic strain change during interdiffusion, therefore annealing temperatures and

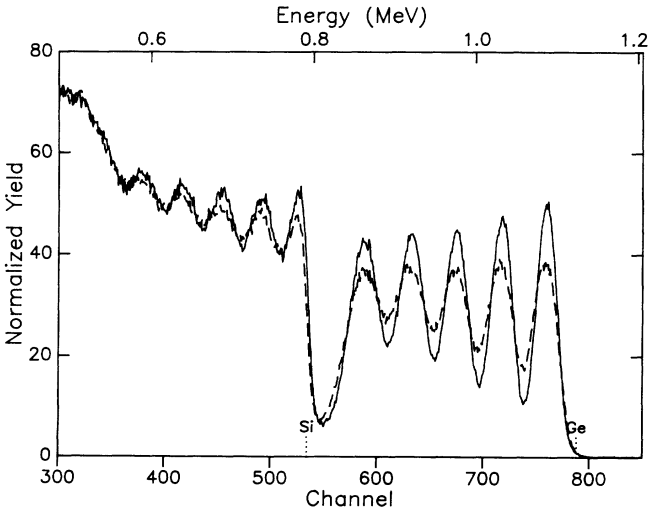

FIG. 2. Grazing-incidence random RBS spectrum of an asymmetrically strained $Si/Si_{0.73}Ge_{0.27}$ superlattice grown on Si(100) before (——) and after (— — —) rapid thermal annealing at 1025 °C for 100 s, showing both the Si and Ge oscillations.

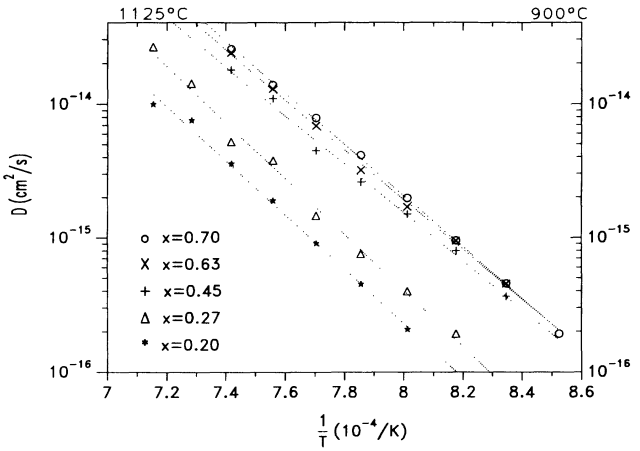

FIG. 3. Arrhenius plot of the diffusion coefficients obtained from asymmetrically strained superlattices with different Ge concentrations.

times were carefully adjusted in precursor experiments such that the diffusion length was nearly the same for samples with identical Ge concentrations. This is an important point, because otherwise the strain and concentration dependence may affect the evaluation of the activation energy for interdiffusion.[15,32] The interdiffusion coefficients obtained from several asymmetrically strained $Si/Si_{1-x}Ge_x$ superlattices grown on Si(100) are shown in the Arrhenius plot of Fig. 3. The interdiffusivity increases by about an order of magnitude with increasing Ge concentration. Activation energies and preexponential factors obtained from the different asymmetrically strained superlattices are summarized in Table I.

Channeling spectra along the [100] sample normal were measured to get information about the presence of crystal defects due to strain relaxation. Two [100] channeling spectra of the $x=0.27$ and 0.63 samples grown on Si(100) are shown together with the corresponding random spectra in Fig. 4. The minimum-yield value of $\chi_{min}\sim 4\%$ determined close to the Si-surface peak of the $x=0.27$ superlattice indicates a low dislocation density. Also, the asymmetrically strained superlattices with $x=0.20$ and 0.45 showed small χ_{min} values, whereas the samples with Ge concentrations $x=0.63$ and 0.70 have considerably larger channeling yields. This can be ascribed to strain relaxation by dislocation formation, since the critical thicknesses[25] for pseudomorphic layer growth are exceeded. The constant slope of the channeling spec-

TABLE I. Preexponential factors and activation energies of interdiffusion obtained for the different asymmetrically strained superlattices.

Ge at. % x	Preexponential factor D_0 (cm²/s)	Activation energy E_a (eV)
0.20	3.4	4.0±0.2
0.27	20.4	4.1±0.2
0.45	0.4	3.6±0.2
0.63	1.3	3.7±0.2
0.70	4.2	3.8±0.2

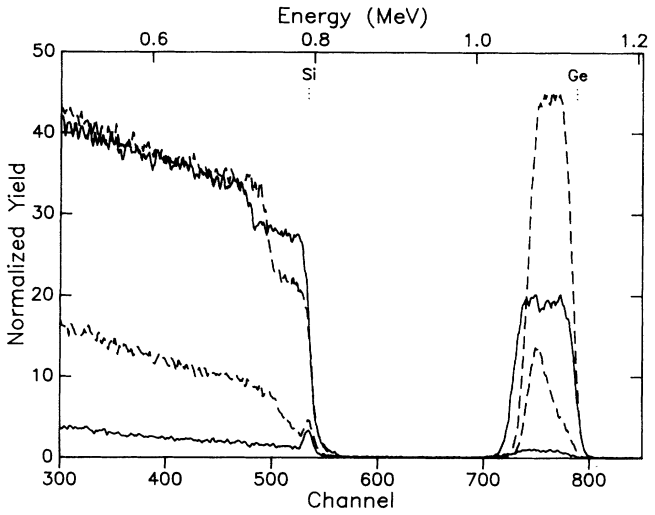

FIG. 4. Random and [100]-aligned RBS spectra of two asymmetrically strained $Si/Si_{0.73}Ge_{0.27}$ (——) and $Si/Si_{0.37}Ge_{0.63}$ (— — —) superlattices. The low χ_{min} value (3.7%) of the $Si/Si_{0.73}Ge_{0.27}$ indicates a high crystalline perfection. The channeling yield of the $Si/Si_{0.37}Ge_{0.63}$ superlattice is considerably higher because the critical-layer thickness is exceeded.

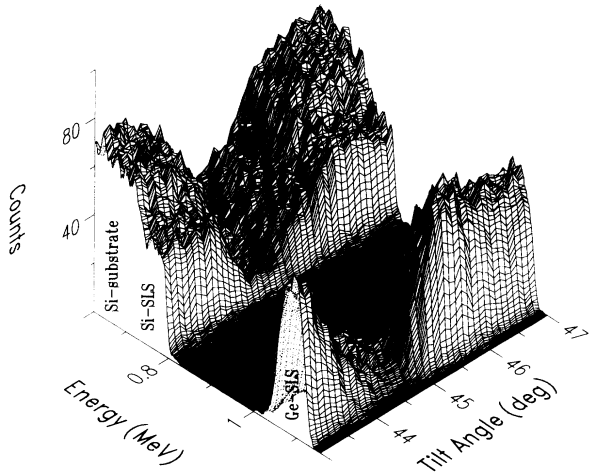

FIG. 5. Angular dependence of the backscattering yield. The shift between the midpoints of the Si and Ge angular scans indicates a nearly pseudomorphic layer growth of the $Si/Si_{0.55}Ge_{0.45}$ sample.

trum of the $x=0.63$ sample in the superlattice region points to nearly homogeneous defect density. No additional defect peak or step is visible at the substrate-superlattice interface, indicating strain relaxation at the interfaces between the adjacent layers of the superlattice.

Channeling angular-yield scans were measured to determine the tetragonal strain in the superlattices.[29] Due to the tetragonal strain, the angle between the sample normal and the inclined [110] direction is no longer 45°, but smaller in the case of compressive strain and larger for tensile strain, respectively. This deviation can be determined by measuring the angular dependence of the backscattering yield along a (100) plane through a [110] crystal axis, as shown for the $x=0.45$ superlattice in Fig. 5. The minimum at the front edge of the Ge signal, which corresponds to the uppermost $Si_{0.55}Ge_{0.45}$ layer, is shifted by $-0.75\pm0.05°$ with respect to the substrate minimum at 45.00°. This value is in good agreement with the theoretical value of $-0.85°$, as calculated on the basis of the biaxial strain model,[33] indicating nearly coherent growth. A significantly larger discrepancy between the measured angular deviation and the theoretical value and the larger χ_{min} values suggest significant strain relaxation in superlattices with Ge concentrations $x>0.45$.

Strain relaxation due to interdiffusion was observed in all samples. Interdiffusion between the individual layers causes a decrease of the concentration gradient and, therefore, leads to strain relaxation. Strain relaxation by formation of defects was only observed in asymmetrically strained superlattices with $x=0.27$ and 0.45. These superlattices show a pronounced increase of the [100] channeling yield at the interface between the superlattice and the Si(100) substrate, which is shown in Fig. 6 for the $x=0.27$ superlattice after rapid thermal annealing (RTA) at 1075 °C for 25 s. This effect may be interpreted as a relaxation of the complete superlattice with respect to the substrate by the formation of dislocations at the interface between the substrate and the superlattice, similar to the observations reported by Bean.[26] The asymmetrically strained superlattices with larger Ge concentrations have already exceeded the critical thickness by formation of dislocations during growth. These superlattices already have a high dislocation density in the as-grown state. No further increase of the dislocation density has been observed by channeling measurements.

To investigate the dependence of interdiffusion on the strain distribution, we analyzed similar superlattices,

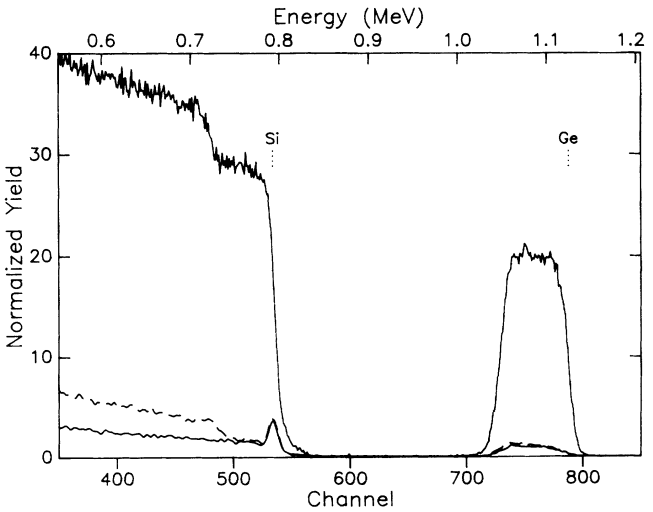

FIG. 6. Random and [100]-aligned RBS spectra of an asymmetrically strained $Si/Si_{0.73}Ge_{0.27}$ superlattice before (——) and after RTA (— — —). The increase of the channeling yield after RTA indicates the formation of crystal defects at the substrate-superlattice interface.

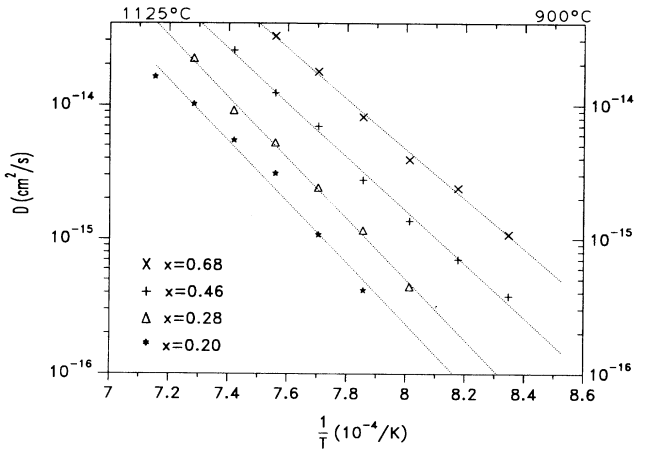

FIG. 7. Arrhenius plot of the diffusion coefficients obtained from symmetrically strained superlattices with different Ge concentrations grown on $Si_{1-y}Ge_y$ buffer layers.

grown on relaxed $Si_{1-y}Ge_y$ buffer layers to obtain a symmetrical strain distribution with tensile strain in the Si layers and compressive strain in the $Si_{1-x}Ge_x$ layers. The interdiffusion coefficients obtained from the symmetrically strained superlattices are shown in Fig. 7. Detailed data are given in Table II.

DISCUSSION

The interdiffusion coefficients shown in Fig. 3, obtained from the asymmetrically strained superlattices with constant Ge concentration x, follow an Arrhenius law indicating the same diffusion mechanism throughout the whole investigated temperature range. The interdiffusion is significantly enhanced with increasing Ge concentration. A comparison between the results of the pseudomorphic superlattice with $x=0.45$ and the relaxed superlattice with $x=0.63$ reveals no significant influence of strain relaxation or defect formation on the interdiffusion. Both the absolute interdiffusion coefficients and the activation energies (given in Table I) of these two particular superlattices are very similar. Surprisingly, early work on Ge self-diffusion in polycrystalline samples exhibited no grain-boundary contributions to the interdiffusivity.[34] Our observations are in agreement with results of van IJzendoorn *et al.*[19] indicating no influence of defects on the interdiffusion. The pure misfit segments of the dislocations are confined to the interface between individual layers and, therefore, should not provide a short-circuit path for diffusion perpendicular to the surface. The only way would be short circuit due to the threading segments of the dislocations. Threading dislocation densities are usually in the order of $10^9/cm^2$,[35,36] giving a mean dislocation distance of about 3000 Å. This dislocation distance is large compared to the layer thicknesses (100 Å) and the diffusion length. However, a diffusion along threading dislocations cannot be excluded from the experimental data because of the lateral spatial averaging of the RBS beam spot.

TABLE II. Preexponential factors and activation energies of interdiffusion obtained for the different symmetrically strained superlattices.

Ge at. % x	Preexponential factor D_0 (cm²/s)	Activation energy E_a (eV)
0.20	350	4.5±0.2
0.28	580	4.4±0.2
0.46	16	4.0±0.2
0.68	4	3.7±0.2

A strong dependence of the Ge tracer diffusion on the Ge concentration was observed already in polycrystalline $Si_{1-x}Ge_x$ alloys.[37] Also, investigations of buried, single-$Si_{1-x}Ge_x$ layers indicated a significant enhancement of the interdiffusion for higher Ge concentrations.[15] The interdiffusion coefficients obtained from the asymmetrically and symmetrically strained superlattices (Figs. 3 and 7) exhibit a similar dependence on the Ge concentration. These results indicate that the influence of the strain distribution on interdiffusion is only of minor importance in comparison with the concentration dependence. Only the symmetrically strained superlattice with a Ge concentration of $x=0.68$ shows a considerably larger interdiffusion as compared with the corresponding symmetrically strained superlattice. As pointed out above, dislocation effects seem to be negligible. The measured activation energies are comparable to those reported by Prokes and Wang,[18] who obtained an activation energy of 4.4 eV in (40-Å $Si_{0.65}Ge_{0.35}$/120-Å Si) superlattices by x-ray diffraction. This is in contrast to interdiffusion studies on ultrathin Si/Ge strained-layer superlattices, composed of alternating monolayers of pure Ge and Si with periods of 16–60 Å, providing an activation energy of about 3.1 eV, a value close to the Ge impurity diffusion in Si.[16,17]

The interdiffusion coefficient D^* in the case of a binary system is given by the Darken equation $D^*=\gamma[c_{Ge}D_{Si}+(1-c_{Ge})D_{Ge}]$, where c_{Ge}, D_{Si}, and D_{Ge} denote the Germanium concentration and the Si and Ge tracer diffusion coefficients in the alloy, respectively, and γ the thermodynamic factor.[32,38] For ideal solutions, such as the isomorphous Si-Ge system, γ is equal to unity. Comparison of experimental data with the Darken equation is impeded by the lack of Si diffusion measurements in Si-Ge alloys. There are numerous studies of Si and Ge self-diffusion,[39,40] of Ge diffusion in Si,[39,41–43] of Si diffusion in Ge,[44] and of Ge tracer diffusion in Si-Ge alloys,[37] but to our knowledge no measurements of Si tracer diffusion in Si-Ge alloys have been reported in the literature.

The activation energies obtained from the symmetrically strained superlattices (Table II) exhibit a decrease with increasing Ge concentration. This tendency is in accord with theoretical calculations of Antonelli and Bernholc[45] on the self-diffusion in strained Si. These calculations compare the activation energies for the formation of neutral tetrahedral interstitials and neutral vacancies in pseu-

domorphic, tensilely strained Si layers on $Si_{1-x}Ge_x$. These conditions are similar to the investigated symmetrically strained superlattices, where the Si layers are also under tensile strain. The calculations show a significant decrease of the activation energy for the formation of interstitials in strained Si from 4.2 to 3.5 eV between growth on pure Si and on pure Ge, but the formation energy of vacancies is independent on the strain. In conjunction with these theoretical investigations, our results suggest a diffusion mechanism by interstitials.

Strain relaxation due to interdiffusion was observed in all samples. An increase of the [100] channeling yield, as shown in Fig. 6, was only observed in asymmetrically strained superlattices with Ge concentrations of $x = 0.27$ and 0.45 at the interface between the superlattice and the Si substrate, which can be attributed to the formation of defects. This behavior is completely different from the asymmetrically strained superlattices with overcritical thicknesses (Fig. 4), which exhibit a continuous increase of the channeling yield in the superlattice. Because of the steplike increase of the channeling yield at the substrate-superlattice interface, we assume that the complete superlattice structure relieves its strain by shearing as a unit with respect to the substrate during annealing.

CONCLUSIONS

Interdiffusion in both symmetrically and asymmetrically strained $Si_{1-x}Ge_x/Si$ superlattices was measured by Rutherford backscattering spectrometry in grazing-incidence geometry. Quantitative interdiffusion coefficients were obtained from the evaluation of the decrease of the modulation amplitudes of the backscattering yield after RTA in the temperature range between 900 °C and 1125 °C. For a given Ge concentration, the temperature dependence of the interdiffusion coefficients follows an Arrhenius law. In both the symmetrically and asymmetrically strained superlattices the interdiffusivity is strongly enhanced for higher Ge concentrations. The influence of strain on the interdiffusion is small in comparison to the concentration dependence. The small decrease of the activation energy with increasing Ge concentration in the case of the symmetrically strained superlattices is compatible with theoretical calculations of the self-diffusion in tensilely strained Si.[45] No significant dependence of the interdiffusion coefficients on the presence of dislocations in relaxed structures was observed. The average activation energy for interdiffusion is about 4.0 eV.

[1]D. B. Noble, J. L. Hoyt, J. F. Gibbons, M. P. Scott, S. S. Ladermann, S. J. Rosner, and T. I. Kamins, Appl. Phys. Lett. **55**, 1978 (1989).

[2]M. L. Green, D. Brasen, H. Temkin, R. D. Yadvish, T. Boone, L. C. Feldman, M. Geva, and B. E. Spear, Thin Solid Films **184**, 107 (1990).

[3]M. L. Green, B. E. Weir, D. Brasen, Y. F. Hsieh, G. Higashi, A. Feygenson, L. C. Feldman, and R. L. Headrick, J. Appl. Phys. **69**, 745 (1991).

[4]G. Abstreiter, Thin Solids Films **183**, 1 (1989).

[5]R. Zachai, K. Eberl, G. Abstreiter, E. Kasper, and H. Kibbel, Phys. Rev. Lett. **64**, 1055 (1990).

[6]E. A. Montie, G. F. A. van de Walle, D. J. Gravesteijn, A. A. van Gorkum, and C. W. T. Bulle-Lieuwma, Appl. Phys. Lett. **56**, 340 (1990).

[7]Y. J. Mii, Y. H. Xie, E. A. Fitzgerald, Don Monroe, F. A. Thiel, B. E. Weir, and L. C. Feldman, Appl. Phys. Lett. **59**, 1611 (1991).

[8]F. Schäffler, D. Többen, H.-J. Herzog, G. Abstreiter, and B. Holländer, Semicond. Sci. Technol. **7**, 260 (1992).

[9]R. Hull, J. C. Bean, J. M. Bonar, G. S. Higashi, K. T. Short, H. Temkin, and A. E. White, Appl. Phys. Lett. **56**, 2445 (1990).

[10]H. Kanaya, K. Fujii, Y. Cho, Y. Kumagai, F. Hasegawa, and E. Yamaka, Jpn. J. Appl. Phys. **29**, L2143 (1990).

[11]R. Hull, J. C. Bean, D. J. Werder, and R. E. Leibenguth, Phys. Rev. B **40**, 1681 (1989).

[12]W. Wegscheider, K. Eberl, G. Abstreiter, H. Cerva, and H. Oppolzer, Appl. Phys. Lett. **57**, 1496 (1990).

[13]P. Y. Timbrell, J. M. Baribeau, D. J. Lockwood, and J. P. McCaffrey, J. Appl. Phys. **67**, 6292 (1990).

[14]R. Hull and J. C. Bean, Appl. Phys. Lett. **55**, 1900 (1989).

[15]G. F. A. van de Walle, L. J. van IJzendoorn, A. A. van Gorkum, R. A. van den Heuvel, A. M. L. Theunissen, and D. J. Gravesteijn, Thin Solid Films **183**, 183 (1989).

[16]S. J. Chang, V. Arbet, K. L. Wang, R. C. Bowman, P. M. Adams, D. Nayak, and J. C. S. Woo, J. Electron. Mater. **19**, 125 (1990).

[17]S. J. Chang, K. L. Wang, R. C. Bowman, and P. M. Adams, Appl. Phys. Lett. **54**, 1253 (1989).

[18]S. M. Prokes and K. L. Wang, Appl. Phys. Lett. **56**, 2628 (1990).

[19]L. J. van IJzendoorn, G. F. A. van de Walle, A. A. van Gorkum, A. M. L. Theunissen, R. A. van den Heuvel, and J. H. Barrett, Nucl. Instrum. Methods B **50**, 127 (1990).

[20]G. F. A. van de Walle, L. J. van IJzendoorn, A. A. van Gorkum, R. A. van den Heuvel, and A. M. L. Theunissen, Semicond. Sci. Technol. **5**, 345 (1990).

[21]S. S. Iyer and F. K. LeGoues, J. Appl. Phys. **65**, 4693 (1989).

[22]B. Holländer, S. Mantl, B. Stritzker, and R. Butz, Nucl. Instrum. Methods B **59/60**, 994 (1991).

[23]J. H. van der Merwe, Surf. Sci. **31**, 198 (1972).

[24]J. W. Matthews and A. E. Blakeslee, J. Cryst. Growth **27**, 118 (1974).

[25]R. People and J. C. Bean, Appl. Phys. Lett. **47**, 322 (1985); **49**, 229(E) (1986).

[26]J. C. Bean, in *Silicon Molecular Beam Epitaxy*, edited by E. Kasper and J. C. Bean (CRC, Boca Raton, FL, 1987).

[27]J. C. Bean, J. Vac. Sci. Technol. B **4**, 1427 (1986).

[28]S. Mantl, E. Kasper, and H. J. Jorke, in *Heteroepitaxy on Silicon II*, edited by J. C. C. Fan, J. M. Phillips, and B.-Y. Tsaur, MRS Symposia Proceedings No. 91 (Materials Research Society, Pittsburgh, 1987), p. 305.

[29]S. T. Picraux, W. K. Chu, W. R. Allen, and J. A. Ellison, Nucl. Instrum. Methods B **15**, 314 (1986).

[30]K. Röll and W. Reill, Thin Solid Films **89**, 221 (1982).

[31]L. R. Doolittle, Nucl. Instrum. Methods B **15**, 277 (1986).

[32]A. L. Greer, in *Diffusion Phenomena in Thin Films and Microelectronic Materials*, edited by D. Gupta and P. S. Ho (Noyes, Park Ridge, NJ, 1988).

[33]M. Murakami, CRC Crit. Rev. Solid State Mater. Sci. **11**, 317

(1983).
[34]H. Widmer and G. R. Gunther-Mohr, Helv. Phys. Acta **34**, 635 (1961).
[35]E. P. Kvam and F. Namavar, Appl. Phys. Lett. **58**, 2357 (1991).
[36]B. Holländer, S. Mantl, B. Stritzker, F. Schäffler, H.-J. Herzog, and E. Kasper, Appl. Surf. Sci. **50**, 450 (1991).
[37]G. L. McVay and A. R. DuCharme, Phys. Rev. B **9**, 627 (1974).
[38]B. Tuck, *Introduction to Diffusion in Semiconductors* (Peregrinus, London, 1974).
[39]G. Hettich, H. Mehrer, and K. Maier, in *Defects and Radiation Effects in Semiconductors,* edited by J. H. Albany (Institute of Physics and Physical Society, London, 1979).
[40]N. A. Stolwijk, M. Perret, and H. Mehrer, Def. Diff. Forum **59**, 79 (1988).
[41]G. L. McVay and A. R. DuCharme, J. Appl. Phys. **44**, 1409 (1973).
[42]M. Ogino, Y. Oana, and M. Watanabe, Phys. Status Solidi A **72**, 535 (1982).
[43]P. Dorner, W. Gust, B. Predel, U. Roll, A. Lodding, and H. Odelius, Philos. Mag. A **49**, 557 (1984).
[44]J. Räisänen, J. Hirvonen, and A. Antilla, Solid-State Electron. **24**, 333 (1981).
[45]A. Antonelli and J. Bernholc, in *Impurities, Defects and Diffusion in Semiconductors: Bulk and Layered Structures,* edited by D. J. Wolford, J. Bernholc, and E. E. Haller, MRS Symposia Proceedings No. 163 (Materials Research Society, Pittsburgh, 1990), p. 523.

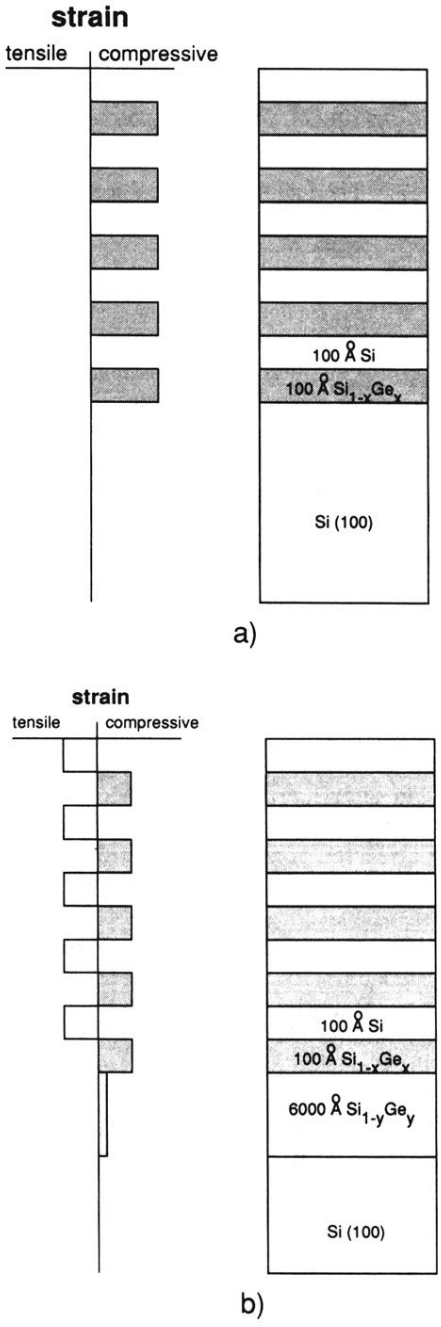

FIG. 1. Scheme of the structure and strain distribution of the investigated (a) asymmetrically and (b) symmetrically strained superlattices.

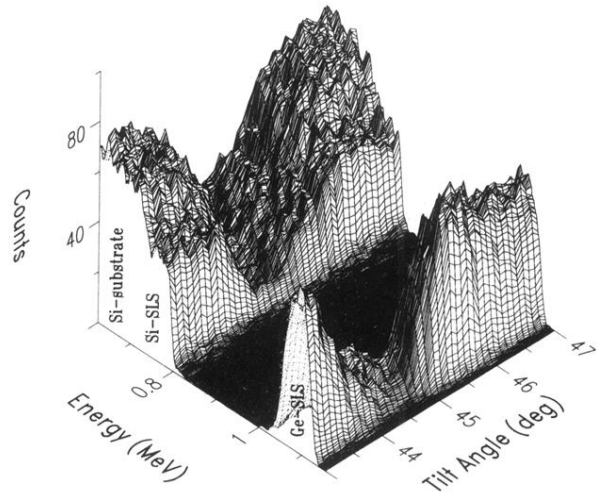

FIG. 5. Angular dependence of the backscattering yield. The shift between the midpoints of the Si and Ge angular scans indicates a nearly pseudomorphic layer growth of the $Si/Si_{0.55}Ge_{0.45}$ sample.